© 2019 IJSRST | Volume 6 | Issue 1 | Print ISSN: 2395-6011 | Online ISSN: 2395-602X
Themed Section: Science and Technology

Optical Study of Electrodeposited Vanadium Oxide Thin Films: Effect of Deposition Time

R. S. Gaikwad*
Vidnyan Mahavidyalaya, Sangola, Tal-Sangola, Dist-Solapur, Maharashtra, India
***Corresponding Author's E-mail:rsgchem@gmail.com**

ABSTRACT
Vanadium oxide thin films were prepared by potentiostatic mode of electrodeposition method. X-ray diffraction study confirms formation of vanadium oxide thin film. Surface morphological study was carried out with the help of Scanning Electron Microscopy. Structural and morphological analyses revealed that the deposited vanadium oxide is polycrystalline in nature with porous nanostructure. The effect of deposition time on optical properties was studied by means of UV-Visible absorption spectroscopy. The UV-Visible absorption spectroscopy reveals that the films deposited at lower deposition times show a relatively low degree of optical absorption, while the spectral absorbance of the films increases with the increase in deposition time. From Tauc's plot, the calculated values of forbidden energy gap E_g vary from 2.33 eV to 2.54 eV.
Keywords: Electrodeposition, Vanadium oxide, thin films, UV-Visible absorption spectroscopy, forbidden energy gap

Introduction:
Vanadium oxides tuning their phase from semiconductor to metal and hence they have flexibility to tune electrical resistivity and optical absorbance. Due to this researchers have taken efforts to use vanadium oxides in variety of applications like optical switching, high capacity lithium batteries, and smart windows for solar cell and optoelectronic devices [1-4]. Vanadium pentoxide (V_2O_5) is the most stable vanadium oxides and because of orthorhombic structure it exhibits anisotropic electric and optical properties [5-6]. The optical properties of vanadium oxide thin films are generally depending upon films crystalline nature, surface morphology and thickness etc. So, basically all these things are connecting to numerous synthesis parameters.
Researcher across globe made efforts to optimize the deposition parameters to receive best quality film with superior phase transition performance, through some physical methods, like magnetron sputtering, molecular beam epitaxy (MBE), sol gel, pulsed laser deposition (PLD) and post annealing [7-10]. But, preparation of vanadium oxide thin film by physical method requires highly sophisticated instruments. Also, maintaining the experimental conditions during the preparation is a hard task. So, the alternative way is to use chemical methods for synthesis of vanadium oxide thin films. Most preferred chemical methods includes electrochemical deposition [11], chemical vapour deposition [12], hydrothermal growth [13] and sol–gel [14] etc. Amongst chemical methods, electrodeposition has some special advantages over others like easy synthesis, not required sophisticated instruments etc.
Bahgat and et al. [15] have reported electrical and optical properties of highly oriented nanocrystalline vanadium pentoxide. They have reported direct and indirect band gap of vanadium oxide thin films as 2.22 eV and 0.27 eV, respectively. Dultsev and et al. [16] have reported structural and optical properties of vanadium pentoxide films prepared by sol-gel method. They have reported that thickness of film affects the optical band

gap energy of vanadium oxide films. The shift of the optical band gap is assigned to change in the stoichiometric composition of the film.

In this paper we present an inexpensive and easy-to-process electrodeposition method to produce vanadium oxide thin film. An effort has been taken to study effect of deposition time on optical properties of electrodeposited Vanadium Oxide thin films.

2. Experimental details:

2.1 Film deposition:

We have deposited vanadium oxide thin films using two electrode systems. In two electrode system of electrodeposition, working electrodes were stainless steel (SS304) and ITO coated glass substrate and counter electrode was graphite. The deposition bath was maintained at constant temperature of 333 K. We have prepared a deposition bath consisting of vanadyl sulphate for the electrodeposition of vanadium oxide thin film electrodes on stainless steel and ITO coated glass substrates. The pH of the bath was adjusted by adding few drops of concentrated HNO_3. To obtain good quality of vanadium oxide thin film, we have optimized preparative parameters like precursor concentration, deposition potential and temperature. All other rest of the deposition parameters are kept constant during the experiment, mentioned in Table1. After deposition films were rinsed with distilled water to remove excessive growth of the film and kept for drying in air. The dried film is used for characterizations.

Table 1: Optimized parameters

Details	Optimized values
Mode	Electrodeposition
Deposition Potential	1.5 V
Bath composition	0.05 M $VOSO_4.H_2O$ + few drops of concentrated HNO_3
pH	~ 3
Deposition bath (medium)	Aqueous
Deposition time	(a) 2 min; (b) 4 min; (c) 6 min.
Temperature	333 K
Substrate	Stainless steel and ITO coated glass

2.2 Characterization techniques:

Crystal structure of the electrodeposited vanadium oxide thin films was studied by using XRD in the range of diffraction angle 2θ from 20–80^0 by using Rigaku D/max 2550Vb+ 18 kw with Cuk$_\alpha$ diffractometer. The SEM images were used to study the surface morphology of the vanadium oxide thin film. UV-Visible absorption study of vanadium oxide thin films was studied by UV-Visible absorption spectrometer.

3. Result and discussion

3.1 X-Ray diffraction study:

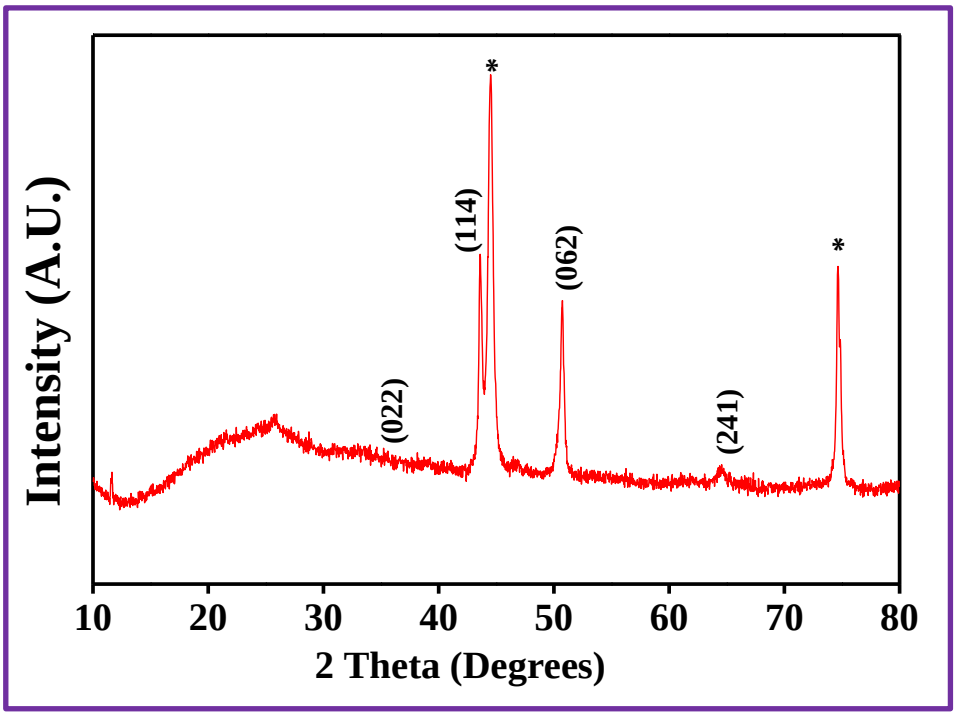

Figure 1: XRD pattern of electrodeposited vanadium oxide thin film deposited at 6 min.

Figure 1 illustrates XRD pattern of vanadium oxide thin film deposited at 6 min. The XRD pattern exhibited four broad peaks, which appear at 2θ values of 34°, 44°, 50° and 65°. The diffraction peaks matches with the standard data (JCPDS: 41-1426). According to the standard diffraction data (JCPDS: 41-1426), these diffraction peaks correspond respectively to the (022), (114), (062) and (241) planes of an orthorhombic structure of vanadium oxide. From Figure 1, it is observed that the deposited vanadium oxide is in polycrystalline in nature. The electrodeposited vanadium oxide thin film does not show any additional peaks, which indicates no secondary phase was formed. The average crystallite size of the vanadium oxide thin film was estimated from the full width at half maximum (FWHM) according to the (062) plane using Debye- Scherrer equation (1) [17]:

$$D = \frac{0.9\lambda}{\beta.\cos\theta} \quad \text{------ (1)}$$

Where, λ is the X-ray wavelength, β is the full width at half maximum of the XRD peak and θ is the Bragg diffraction angle. The calculated value of crystallite size was found to be 10 nm.

3.2 Surface morphological study:

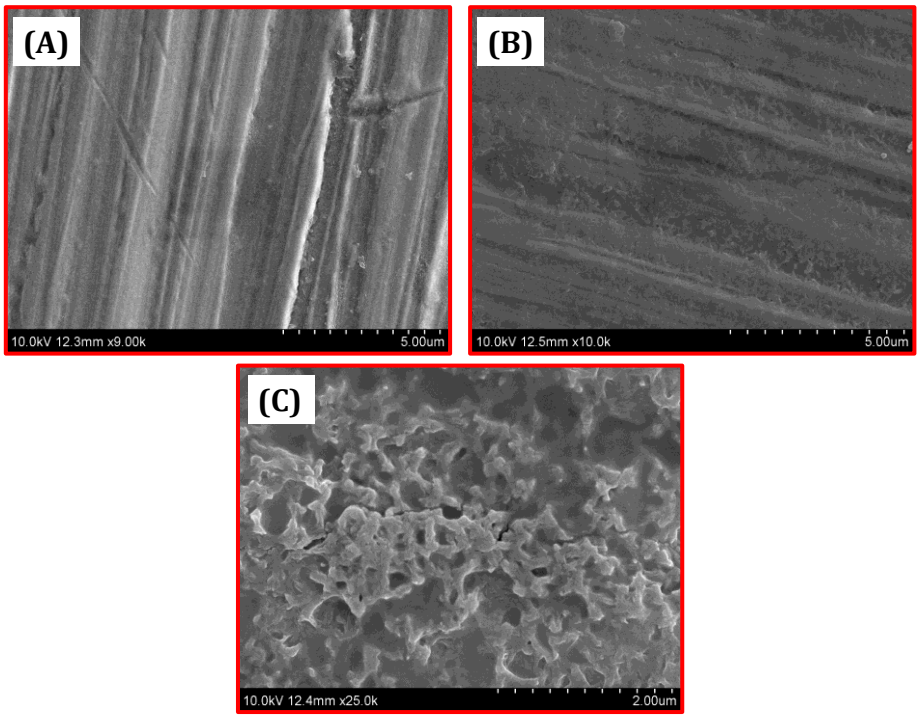

Figure 2: SEM images of electrodeposited vanadium oxide thin films for film deposited at a) 2 min; b) 4 min and c) 6 min.

The surface morphologies of the vanadium oxide thin films obtained with different deposition times at 333 K were determined by using scanning electron microscopy (SEM) and are shown in Fig. 2. When the SEM images of the films were examined, it was observed that as electrodeposition time increased from 2 min to 6 min, the number of coalescence in the film increased and further surface area of substrate covered. At the same time as, it was observed that because of the clusters collections (ion-by-ion mechanism) and clusters growth (cluster-by-cluster mechanism) on the surface of substrate a porous structure formed. These results are in good agreement with the literature. Guneri and et al [18] have reported that effect of deposition time on structural, electrical, and optical properties of SnS thin films deposited by chemical bath deposition. They reported that as deposition time increases the number of aggregations in the film increased and a more homogeneous structure formed.

3.3 UV-Visible absorption spectroscopy:

The spectral absorbance characteristics of electrodeposited vanadium oxide thin films at different deposition times are shown in Figure 3 (A). The curves indicate that the films deposited at lower deposition times show a relatively low degree of optical absorption, while the spectral absorbance of the films increases with the increase in deposition time. The spectral characteristic curves show that the optical absorption decreases with increase in wavelength. The effect of the deposition time on the forbidden energy gap values was calculated by the optical absorbance measurements. The optical absorbance A and the optical absorption coefficient were determined by measuring log (1/T) and using the formula;

$$\alpha = \left(\frac{1}{d}\right)\left[\log\left(1/T\right)\right] = A/d \quad \text{----- (2)}$$

Where T is the transmittance and d is the film thickness. Fig. 3 (A) shows the optical absorbance of the films deposited at a) 2 min, b) 4 min and c) 6 min. Fig. 3(B) shows the Tauc's plot of the films deposited at a) 2 min, b) 4 min and c) 6 min. The optical absorption coefficient α as a function of photon energy hν is given as

$$\alpha h\nu = B\left(h\nu - E_g\right)^n \quad \text{-------- (3)}$$

where n is an exponent, ν is the frequency of the incident photon, h is the Plank's constant, B is a constant, and Eg is the forbidden energy gap of the material. The exponent n can take the values 2, 3, ½ and 3/2 for indirect allowed, indirect forbidden, direct allowed and direct forbidden transitions, respectively [19-22]. Plotting of $(\alpha h\nu)^2$ versus (hν) and extrapolating to $(\alpha h\nu)^2=0$ gives the value of E_g. The calculated E_g values vary from 2.33 eV to 2.54 eV.

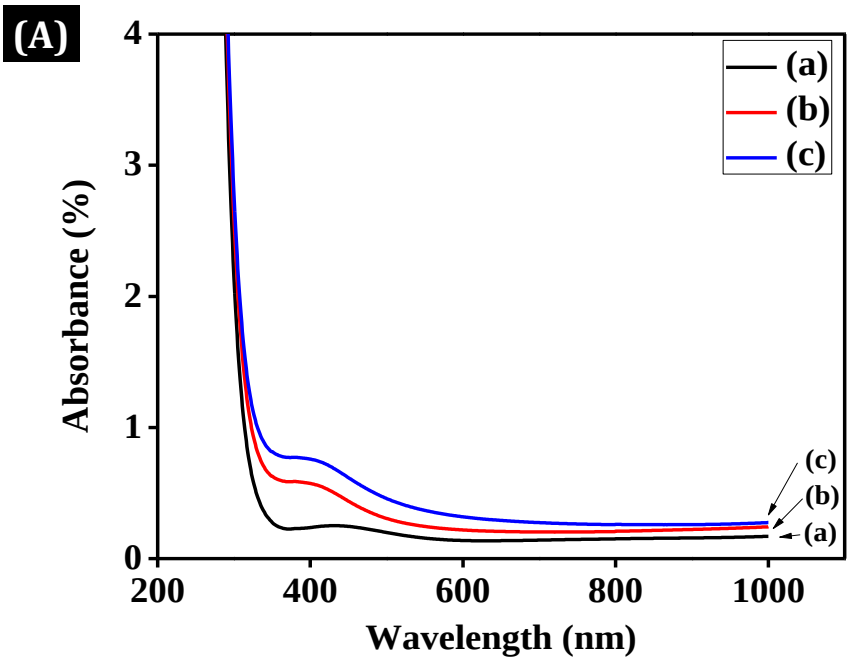

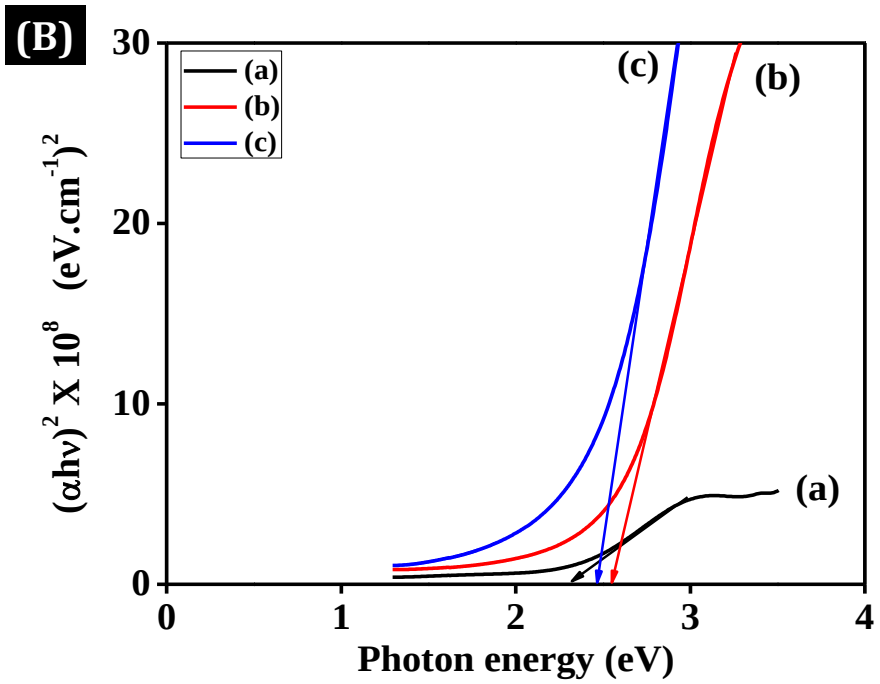

Figure 3: (A) UV-Visible absorption spectra of films deposited at a) 2 min, b) 4 min and c) 6 min; (B) Tauc's plot for films deposited at a) 2 min, b) 6 min and c) 8 min;

Conclusions

In summary, we have successfully deposited vanadium oxide thin film by low cost and simple method i.e. potenetiostatic mode of electrodeposition. By varying deposition time between 2 min to 6 min, may alter the structural, morphological and optical properties of vanadium oxide thin films. XRD study confirmed the polycrystalline nature of vanadium oxide thin film. SEM images showed that a porous structure formed due to two types of mechanism as ion-by-ion mechanism and cluster-by-cluster mechanism on the surface of substrate. From UV-Visible absorption study it is observed that the spectral absorbance of the films increases with the increase in deposition time.

Acknowledgements: One of the authors RSG is very much grateful to Dr. S. M. Mane for providing characterization facilities.

References:

[1]. S. Beke, L. Ko˝ ro¨ si, S. Papp, L. Na´ nai, A. Oszko´ , J.G. Kiss, V. Safarov, Nd:YAG laser synthesis of nanostructural V2O5 from vanadium oxide sols: Morphological and structural characterizations, Applied Surface Science, 254 (2007) 1363.

[2]. S.P. Lim, J.D. Long, S. Xu, K. Ostrikov, Nanocrystalline vanadium oxide films synthesized by plasma-assisted reactive rf sputtering deposition, Journal of Physics D: Applied Physics, 40 (2007) 1085.

[3]. L.J. Meng, R.A. Silva, H.N. Cui, V. Teixeira, M.P.D. Santos, Z. Xu, Optical and structural properties of vanadium pentoxide films prepared by d.c. reactive magnetron sputtering, Thin Solid Films, 515 (2006) 195.

[4]. X. Wu, F. Lai, L. Lin, Y. Li, L. Lin, Y. Qu, Z. Huang, Influence of thermal cycling on structural, optical and electrical properties of vanadium oxide thin films, Applied Surface Science, 255 (2008) 2840.

[5]. M. Sullivan, T. V. Son, N. Beaudoin and A. Hache, Optical scattering during phase transition of vanadium dioxide, Optics Communication, 356 (2015) 395–399
[6]. R. S. Ingole, B. J. Lokhande, Effect of pyrolysis temperature on structural, morphological and electrochemical properties of vanadium oxide thin films, Journal of Analytical and Applied Pyrolysis, 120 (2016) 434–440
[7]. M. Wang, J. Bian, H. Sun, W. Liu, Y. Zhang, Y. Luo, n-VO2/p-GaN based nitride-oxide heterostructure with various thickness of VO2 layer grown by MBE, Applied Surface Science, 389 (2016) 199–204.
[8]. C.Y. Kang, Z.F. Wei, C. Zhang, S.S. Liang, C.C. Geng, J.B. Wu, H.H. Liu, H.T. Zong, M. Li, Evolution of polymorph and photoelectric properties of VO2 thin films with substrate temperature, Journal of Alloys and Compounds, 803 (2019) 394.
[9]. W. Lu, G. Zhao, B. Song, J. Li, X. Zhang, G. Han, Preparation and thermochromic properties of sol-gel-derived Zr-doped VO2 films, Surface Coating and Technology, 320 (2017) 311.
[10]. Y. Huang, D. Zhang, Y. Liu, J. Jin, Y. Yang, T. Chen, H. Guan, P. Fan, W. Lv, Phase transition analysis of thermochromic VO2 thin films by temperature-dependent Raman scattering and ellipsometry, Applied Surface Science, 456 (2018) 545.
[11]. J. M. Li, K. H. Chang, C. C. Hu, A novel vanadium oxide deposit for the cathode of asymmetric lithium-ion supercapacitors, Electrochemistry Communications, 12 (2010) 1800
[12]. D. Louloudakis, D. Vernardou, E. Spanakis, N. Katsarakis, E. Koudoumas, Thermochromic vanadium oxide coatings grown by APCVD at low temperatures, Physics Procedia, 46 (2013) 137
[13]. Mukherjee, H. A. Ardakani, T. Yi, J. Cabana, R. S. Yassar, R. F. Klie, Direct characterization of the Li intercalation mechanism into α-V2O5 nanowires using in-situ transmission electron microscopy, Applied Physics Letters, 110 (2017) 213903
[14]. Z. Wan, R. B. Darling, A. Majumdar, M. P. Anantram, A forming-free bipolar resistive switching behavior based on ITO/V2O5/ITO structure, Applied Physics Letters, 111 (2017) 041601.
[15]. A. Bahgat, F. A. Ibrahim, M. M. El-Desoky, Electrical and optical properties of highly oriented nanocrystalline vanadium pentoxide, Thin Solid Films, 489 (2005) 68.
[16]. F. N. Dultsev, L. L. Vasilieva, S. M. Maroshina, L. D. Pokrovsky, Structural and optical properties of vanadium pentoxide sol–gel films, Thin Solid Films, 510 (2006) 255.
[17]. Salem, E. Saion, N.M. Al-Hada, H.M. Kamari, A.H. Shaari, S. Radiman, Simple synthesis of ZnSe nanoparticles by thermal treatment and their characterization, Results in Physics, 7 (2017) 1175
[18]. E. Guneri, C. Ulutas, F. Kirmizigul, G. Altindemir, F. Gode, C. Gumus, Effect of deposition time on structural, electrical, and optical properties of SnS thin films deposited by chemical bath deposition, Applied Surface Science, 257 (2010) 1189
[19]. J. Tauc, The optical properties of solids. In:Abeles F, editor. Amsterdam: North-Holland Publ.Co.; 1972 .p.277.
[20]. J. Tauc, R. Grigorovici, A.Vancu, Optical properties and electronic structure of amorphous germanium, Solid State Physics (B), 15 (1966) 627.
[21]. G. A. Khan, C. A. Hogarth, Optical absorption spectra of evaporated V2O5 and co-evaporated V2O5/B2O3 thin films, Journal of Materials Science, 26 (1991) 412.
[22]. R. M. Oksuzoglu, P. Bilgic, M. Yıldırım, O. Deniz, Influence of post-annealing on electrical, structural and optical properties of vanadium oxide thin films, Optics & Laser Technology, 48 (2013)102.

© 2019 IJSRST | Volume 6 | Issue 2 | Print ISSN: 2395-6011 | Online ISSN: 2395-602X
Themed Section: Science and Technology

Review on Ferrites : Structural Magnetic and Electrical Properties

Swati Patil[1], Shankar Dhasade[2]
[1]Pratapsinh Mohite-Patil Mahavidyalaya, Karmala, Maharashtra, India
[2] Vidnyan Mahvidyalaya, Sangola, Maharashtra, India
Corresponding author : Swati D Patil (swatippatil@gmail.com)

ABSTRACT

Researchers are taking extraordinary interest in the preparation and characterization of lithium ferrites due to their wide variety of applications in many fields. lithium ferrites are a class of smooth magnetic materials which have excellent electric, magnetic and optical properties. The properties of lithium ferrites include high cost of resistivity, Permeability, permittivity, saturation magnetization, low power losses and coercivity. The above referred to wonderful features of lithium ferrites make them appropriate for the use in various packages. In medical field these ferrites are used for treatment cancer and MRI. Lithium ferrites are also utilized in electronic applications.

Keywords : Treatment Cancer, MRI. Lithium, Permeability, Permittivity, Saturation Magnetization, Low Power Losses

Introduction:

Ho doped Lithium-Zink ferrites and its dielectric behavior at high frequency and magnetic properties are studied[1] sol–gel synthesized CoFe2-xHoxO4 nano ferrites its structural and physical properties were studied [2] The change in magnetic and structural properties of Gadolinium doped cobalt-zinc ferrites governed by spin rotations and domain wall movement were explained [3] $Co_{0.5}M_{0.3}7Cu0.13Fe_2O_4$ ferrites were studied for its structural, magnetic and electrical behavior, [4] By aloe vera plant-extracted ferrite nanoparticles of MFe_2O_4, M = Ni, Co, Mn, Mg, Zn are prepared [5] zinc ferrite nanoparticles synthesized from Sugarcane juice and its application as degradation of mixed dyes and antibacterial activities are studied[6] Electric and dielectric properties of Neodymium substituted manganese -nikel-zinc are explained[7]

Metal ions substituted cobalt ferrites synthesized by sol–gel auto-combustion route were studied for magnetic properties [8] Nanocrystalline Mn-Zn Ferrites synthesized by microwave assisted method were studied, [9] $NiCr_xFe_{2-x}O_4$ ferrites were studied for its optical, electric, mechanical, and Magnetic properties, [10]

Graphical Abstract: Study of Ferrites

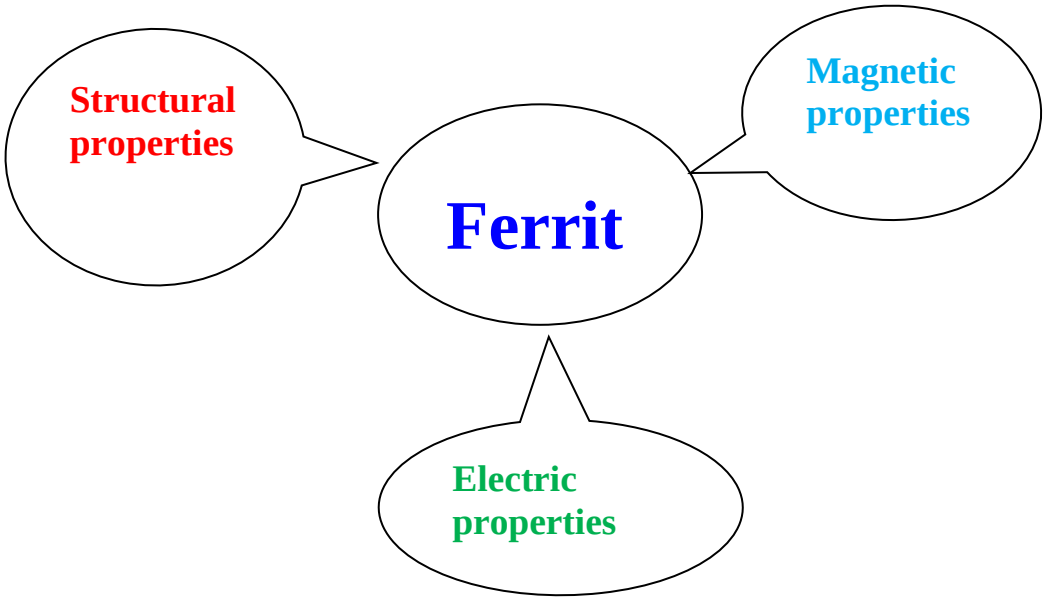

The remanent magnetization and coercivity of the Nanocomposites of hexaferrite became 2 and a 2.5 instances better, respectively by means of adding $BaFe_{11.7}A_{10.15}$ $Zn_{0.15}O_{19}$ section. The Cole-Cole plots of the nanocomposite x=0.4 at the chosen temperatures suggests two successive semicircles at all the selected temperatures. The First low frequencies semicircle elucidates the contribution of the grain boundary and the second, at excessive frequencies, offers the contribution of grain to conduction manner. Multilateral applications for change spring magnets can be manufactured the usage of the ones nanocomposites. These hexaferrite was fabricated by using the citrate–nitrate auto combustion method [11]

Nanoparticles of roughly spherical in shape with size in range of 10–15 nm, are estimated from X-ray diffraction and TEM micrographs with increase in crystal size coresivity increase and decreases with decreases in size of the magnetic particles. The variation in valance states Mn and Fe atoms in $Zn_xMn_{1-x}Fe_2O_4$ is studied. The magnetic properties of $Zn_xMn_{1-x}Fe_2O_4$ will degrade with loss of Zinc is observed. Due to the combined effects of oxygen partial pressure and temperature in the region of 450^0c the phase is not stable for $Zn_xMn_{1-x}Fe_2O_4$.[12]

Humaira Anwar et al. studied, Structural, Electrical and Dielectric Parameters of Mn-Zn Nano Ferrites prepared by the chemical co-precipitation method, changes due to increase of temperature, while the resistivity of ferrite deceases with increases of temperature. Activation energy of the samples was found to be in the range of 0.70 to 0.77eV. Due to agglomeration in of Mn-Zn ferrites Porosity, crystallite Size, resistivity increases and density decreases with increase in temperature. Maximum weight loss is observed up to temperature of 518 K. The dielectric constant decreases rapidly with increase in frequency [13] It is seen that the coercivity value of the all of nanocomposites are decrease than natural hard Phase and for one-pot synthesized nanocomposites, are greater than pure smooth phase. The coercivity reduction in composites organized by using physical Mixing approach is lots astounding and for smooth phase content material better than 50 %.It is decrease than natural pure phase. For high values of the smooth phase, the exchange Force at the soft grains is weakened and dipolar interaction among pure phase.Moments becomes enormous. So, the opposite domains inside the smooth section with Low nucleation area may be nucleated without problems. This could lower the coercivity Of composite [14]. In

addition, whilst the importance of the reverse field is Progressively expanded, the domain partitions of the pure phase flow in the direction of the Interface between the soft and hard phases and could invade into the hard phase Area, which leads to the irreversible magnetization reversal of the hard section. Therefore neighboring grains could purpose additional demagnetizing effect and Bring about the reduction of average coercivity of the composite, as compared to the Pure hard phase [14]. Shuli He et al. explained Maximized precise loss of electricity and intrinsic loss strength drawing near theoretical limits for alternating-current (AC) magnetic-subject heating of nanoparticles are said. That is performed by way of engineering the powerful Magnetic anisotropy barrier of nanoparticles through alloying of hard and soft ferrites. 22 nm $Co_{0.03}Mn_{0.28}Fe_{2.7}O_4/SiO_2$ nanoparticles attain a precise loss power price of 3417 W g^{-1} metallic at a area of 33 kA m^{-1} and 380 kHz [15]. Biocompatible $Zn_{0.3}Fe_{2.7}O_4/SiO_2$ nanoparticles gain particular Loss energy of 500 W g^{-1}Steel and intrinsic loss energy of 26.8 nHm^2 kg^{-1}[15]. At field parameters of 7 kA m^{-1} and 380 kHz, below the medical safety Limit. Magnetic bone cement achieves heating good enough for bone Tumor hyperthermia, incorporating an ultralow dosage of just 1 wt% of nanoparticles[15]. In cell hyperthermia experiments, these nanoparticles exhibit excessive cellular death price at low field parameters. $Zn_{0.3}Fe_{2.7}O_4/SiO_2$ nanoparticles show cellular viabilities above ninety seven% at concentrations up to 500 μg mL^{-1} inside forty eight h, suggesting toxicity lower than that of magnetite[15]. Cristina Ileana Covaliu et al. reported that, biomedical applications magnetic nanoparticles coated with polysaccharide polymers were studied and these microorganisms of as prepared hybrid materials show the non-toxic properties. The magnetic properties of all ferrite nanoparticles and hybrid materials have Shown the super paramagnetic normal behavior, that the saturation magnetization (Ms) values are much decrease than the ones of the corresponding "bulk" ferrite. The lower of Ms might be because of the decrease of the particle sizes[16]. The weak hysteresis might be assigned to the small length of the nanoparticles having a single magnetic domain. In addition, taking into account that at the maximum Losses (eddy currents losses), these substances being aggressive for some medical fields[16]. All Hybrid materials exhibit a decrease saturation magnetization and a decrease susceptibility than the uncoated ferrite nanoparticles due to the decreased content of the magnetic aspect within the composite material however the values are enough excessive for medical programs [16] . Cristina Ileana Covaliu also reported the cobalt ferrite nanoparticles ($CoFe_2O_4$) have a different Conduct: its mixture with polyvinylpyrrolidone (PVP) increases now not only the saturation magnetization, but additionally the hysteresis parameters (coercivity and remanence). An rationalization may be the huge agglomeration of the magnetic nanoparticles that allows the multidomain magnetic structure. He also reported the cobalt ferrite nanoparticles with sizes less than 10 nm have low magnetic reaction skills considering the biomedical applications[17]. As zinc concentration increases the microstructure and relaxation frequency of as synthesized Mn–Zn ferrites changes there is tendency to increase the grain size as the Zn concentration increases, the study also reveals that the average grain sizes of microstructures increases with increasing dwell time[18]

References:

[1]. Alina Manzoora, Muhammad Azhar Khana, Muhammad Yaqoob Khan, Majid Niaz Akhtar,Altaf Hussain, Ceramics International,44(2018) 6321-6329

[2]. K.K. Patankar , D.M. Ghone , V.L. Mathe , S.D. Kaushik , Journal of Magnetism and Magnetic Materials 454 (2018) 71–77

[3]. Anil B. Mugutkar, Shyam K. Gore, Rajaram S. Mane, Khalid M. Batoo, Syed F. Adil,Santosh S. Jadhav, Ceramics International, 44 (2018) 21675-21683

A. Ramakrishna , N. Murali , S.J. Margarette , Tulu Wegayehu Mammo, N. Krishna Joyt, Sailaja , Ch.C. Sailaja Kumari , K. Samatha , V. Veeraiah, Advanced Powder Technology 29 (2018) 2601-2607
[4]. Materials Research Bulletin, Santi Phumying, Sarawuth Labuayai, Ekaphan Swatsitang, Vittaya Amornkitbamrung, Santi Maensiri, 48 (2013) 2060-2065
[5]. S.B.Patil, H.S.Bhojy, Naik, G.Nagaraju, R.Viswanath, S.K.Rashmia, M.Vijay kumar, Materials Chemistry and Physics 212 (2018) 351-362
[6]. W.R.Agami, Physica B: Condensed Matter, 534 (2018) 17-21
[7]. Guoxi Xi Yuebin,Xi , Materials Letters, 164, (2016) 444-448
[8]. Surender Kumar, Tukaram J. Shinde, Pramod N. Vasambekar , Adv. Mat. Lett. 2013, 4(5), 373-377
[9]. S.Bushkova, Ivan P.Yaremiy, Journal of Magnetism and Magnetic Materials, 461 (2018) 37-47
[10].F. Mansour, O. M. Hemeda, M. A. Abdo and W. A. Nada, Journal of Molecular Structure ,1152 (2018) 207-214
[11].Tao Sun, Andrew Borrasso, Bin Liu, Vinayak Dravid, J. Am. Ceram. Soc., 94 [5] (2011)1490–1495
[12].Anwar, Asghari Maqsood, Key Engineering Materials 510-511 (2012) 163-170.
[13].Shahab Torkian, Ali Ghasemi, Reza Shoja Razavi, Journal of Magnetism and Magnetic Materials, 416 (2016) 408-416
[14].Shuli He, Hongwang Zhang, Yihao Liu, Fan Sun, Xiang Yu, Xueyan Li, Li Zhang,Lichen Wang, Keya Mao, Gangshi Wang, Yunjuan Lin, Zhenchuan Han, Renat Sabirianov,and Hao Zeng, Small 2018, 1800135
[15].Cristina Ileana Covaliu , Daniela Berger,Cristian Matei , Lucian Diamandescu , Eugeniu Vasile ,Camelia Cristea , Valentin Ionita , Horia Iovu, J Nanopart Res (2011) 13:6169–6180
[16].Cristina Ileana Covaliu, Ioana Jitaru , Gigel Paraschiv , Eugeniu Vasile , Sorin-Ştefan Biriş, Lucian Diamandescu , Valentin Ionita , Horia Iovu, Powder Technology 237 (2013) 415–426
[17].Zapata, G.Herrera, Ceramics International, 39 (2013) 7853-7860

Cite this Article

Swati Patil, Shankar Dhasade, "Review on Ferrites : Structural Magnetic and Electrical Properties", International Journal of Scientific Research in Science and Technology (IJSRST), Online ISSN : 2395-602X, Print ISSN : 2395-6011, Volume 6 Issue 2, pp. 1008-1011, March-April 2019.

Journal URL : https://ijsrst.com/IJSRST23100110